We would like to sincerely thank the Reviewers for their support and constructive comments on the manuscript. Their comments have helped to improve the quality of our work. We provide here a detailed point-by-point answer (shown in blue), to their comments and suggestions.

Reviewer 1:

The present manuscript presents a complete analysis of O4 and NO2 vertical profiles during three months in Madrid, Spain with the aid of ground-based MAX-DOAS 2-D observations. The aerosol and NO2 vertical profiles in multiple viewing azimuth directions are presented here as well as the horizontal NO2 distribution around the measurement site. Finally, the 2-D MAX-DOAS NO2 near-surface concentrations are compared with the in-situ NO2 measurements in Madrid.

I recommend the publication of the manuscript after consideration of a major number of specific comments:

We thank the reviewer for her/his thorough and constructive comments, which we address below.

Specific comments:

1. Page 1, Line 19: Please write the spatial resolution of the mesoscale events.

We have included the spatial resolution (in the order of a few kilometers) in lines 25-26.

2. Page 1, Line 27: In my understanding, you used one inversion algorithm (not inversion algorithms) for the aerosol and the NO2. Please correct that and write the name of the inversion algorithm that is used (bePRO).

We have changed it by “an inversion algorithm” in line 19 in the abstract.

3. Page 1, Abstract: I would recommend that you write in a more clear way, the main findings of this study and the main contributions/innovations that you have made.

Thank you for this useful comment. We rewrote this part and we included in more detail the main findings of our study, from line 20 to line 24.

4. Page 2, Line 49: I would recommend to write that you have developed two MAX-DOAS instruments and not just MAX-DOAS instruments.

We developed one MAX-DOAS instrument, for this reason we specify now “we have deployed a Multi AXis Differential Optical Absorption Spectroscopy (MAXDOAS) instrument” in lines 63-64.

5. Introduction: It would be valuable to add a paragraph in which you cite previous MAX-DOAS studies of two-dimensional measurements (like Ortega, Schreier, Wang, Dimitropoulou etc.) as well as studies where MAX-DOAS observations are compared with in-situ measurements.

We have added a paragraph (lines 88-93) in which we cite previous studies that report measurement using MAXDOAS-2D instruments.

6. Section 3.2: Where do you expect to measure higher NO2 concentrations (North, South etc.)?

Based on previous studies, there is no clear, steady distribution of NO_2 in Madrid. Instead there are strong spatial gradients and temporal changes (including considerable traffic hot-spots), thus making it difficult to predict with great accuracy how the NO_2 will be distributed at a given time. However, mesoscale simulations in Madrid show that in general, higher NO_2 mixing ratios are expected in the southern part of the city taking into account the population distribution and commuting patterns (see Picornell et al., 2019 for more details). We have included this issue in lines 214-222.

7. Page 7, Line 193: In your study, one complete MAX-DOAS scan takes one hour. The advantage is that you have a very nice horizontal sampling but at the other hand, you risk to measure the same NO2 air mass in multiple azimuthal directions (for example, during one hour, the NO2 that you observe in the North can be moved by the wind in the North East direction). Please add a sentence in which, you make clear the advantages and disadvantages of your choice.

Understood. We have added it in lines 264-271. Indeed, it will be useful for the reader to include the advantages and disadvantages of such measurements setup.

8. Page 11, Line 252: After the filtering of the MAX-DOAS measurements, which is the percentage of accepted scans?

We have included the percentage of cycles (slightly above 90 %) that were considered valid (concerning the quality checks) as input for the RTM. You can see this part in lines 349-352.

9. Page 11, Line 264: The RTM is the forward model and the bePRO is the inversion algorithm. Please correct this.

We have modified this part, (line 356 in our revised manuscript).

10. Page 12, Line 290: It's not exactly an analogous process because for the O4 and aerosol, non-linear calculations are performed and for trace gases as NO2, we have linear calculations. Please verify if it's the case for bePRO and correct or not this sentence.

Thank you for this appreciation. We have clarified that a linear analysis is made to estimate the vertical concentration profile of NO_2 using the light paths derived from the non-linear analysis of the O_4 and aerosol (from line 364 to line 372).

11. Page 13, line 310-318: You have used Standard atmosphere profiles, which are widely used in studies like the present one. But, you should include an uncertainty estimate of using a standard profile instead of a real profile (by meteorological measured data).

We have developed a more detailed uncertainty analysis. We have included the uncertainty sources in the whole analysis from line 482 to line 490. Concerning the use of a given atmospheric profile, we have concluded that the RMS of the relative variations (within the first 10 km height) was of about 8 %. We went a step further and estimated that, regarding the light paths, the RMS of the relative changes coming from the atmospheric profile choice was below 2 %.

12. Section 4.2: You should a paragraph in which you present an average error estimate of the retrievals and add a Table with all the error sources (smoothing error etc).

As described above, we have completed the section with the average uncertainties of the retrieval. A table has been included and appears in the text from line 493 to line 501.

13. Section 4.3: In your results, you should discuss the range of the estimated horizontal distances for the UV and Vis during your measurement period

The range of the estimated horizontal distances appear now in lines 517-519.

14. Figure 6: These results are from which measurement day and scan/hour? I assume that it is not the whole period, right?

Yes, these results are for the entire period, in line 540 it is marked that this correlation is for the entire campaign. We usually do this with the purpose of checking the goodness of the analysis for the entire campaign, it is a useful and rapid way to assess the simulations.

15. Figure 7: How do you explain the aerosol peak at around 50 deg. VAA and in high altitude?

This aerosol peak could come from traffic because there is a main road at this VAA. However, we are not sensitive above the boundary layer to know if this peak could be due to uncertainties in the RTM. Anyway, that would be one of the main ideas of this work: that the O_4 DSCDs are the ones which drive the light path analysis. As shown in Section 4.2, an aerosol loading may cause a quite similar (or even the same) effect as small variations in the atmospheric profiles or parameters. However, this does not affect the light path estimation and the subsequent trace gas analysis, hence only affecting the certainty of assigning an irradiance extinction as aerosol (specially in higher layers), lines 565-569.

16. Page 20, Line 465: Why do you use the UV distance and the Vis which is larger?

We have mentioned in line X that we only take into account the air quality monitor stations which are at a distance from our MAXDOAS equal or lower than 10 km, and the UV light path ranges typically in the order of 8-10 km, hence that is why we chose the NO_2 retrieved in the UV region for the comparison. It appears now in lines 658-662.

17. Figure 10: Please include a 1:1 line and put the same axis limits in both x, y axis in order to quantify rapidly the underestimation on the near-surface NO2 concentrations by the MAX-DOAS

Figure 11 (previously figure 10) has been modified in order to show 1 to 1 axis, so that the underestimation is easier to observe, as you suggest (line 672)

18. Page 21, Line 480: You write that the slope is lower than 1 (it is 0.4) which is true but you should add a sentence in which you discuss this finding. Is it in agreement with previous studies that compared MAX-DOAS and in-situ?

We have completed this part including some previous works in which similar conclusions were reached (we also discuss the slope value from line 686 to line 689).

19. Conclusions: You should make this section larger and discuss more your results

We have now a more complete summary and conclusions part (section 6).

20. Through the whole manuscript, references should be added, as I mentioned in previous comments

Several references have been added through the entire work.

Technical corrections

1. Page 2, line 34: gaseous pollutant concentrations instead of gaseous pollutants concentrations

Changed. Now line 44.

2. Page 3, line 73: path lengths instead of paths lengths

Changed. Now line 99.

3. Page 11, Line 256: inversion algorithm method instead of inversion algorithms.

Changed. Now line 356.

We would like to sincerely thank the reviewer for her/his support and comments on the manuscript. The comments have helped to improve the quality of our work and include some new information.
We provide here a detailed point-by-point answer (shown in blue), to the comments and suggestions.

Reviewer 2:

In their manuscript “Two-dimensional monitoring of air pollution in Madrid, Spain using a MAXDOAS-2D instrument”, the authors report on measurements in Madrid using a new MAX-DOAS instrument with both elevation and azimuth pointing capabilities. Examples of NO2 profile retrievals are discussed and some results of onion peelingretrievals presented. Finally, a comparison is performed between hourly mean values from the lowest MAX-DOAS profile level and data from the air quality network, showing good correlation. The manuscript is generally clear and well written but lacks detail in many places. It also does not provide reference to the many existing studies using similar instruments, performing similar retrievals, and addressing similar research questions.

My main problem with this manuscript is however the lack of novelty: In fact, I do not see anything new in this manuscript on instrument development, DOAS retrievals, profile retrievals, the onion peeling approach or the validation of the retrievals. The instrument is similar to many others operated (see Kreher et al., 2020), the DOAS retrieval is performed using the freely available software QDOAS, the profile retrieval is using the software BePro, the onion peeling follows the work by Ortega et al. And the validation is limited to a single figure showing measurements from a not further defined time period. I therefore unfortunately cannot recommend this manuscript for publication in Atmospheric Measurement Techniques.

The measurements of the 2d-MAX-DOAS instrument in Madrid certainly have the po-tential to provide interesting results on

pollution in the city, and how it depends on emissions and meteorology. Such a study would then however be more appropriate for ACP than for AMT.

I also have some more detailed comments, which the authors could take into consideration when using the existing draft as base for another manuscript providing novel results and data.

We thank the reviewer for her/his comments, which we address below. We however think that AMT is the appropriate journal for publication of our results. To further add information on the capabilities of MAXDOAS-2D to the study of air pollution in Madrid, we have performed, and included in the revised manuscript, analysis of HONO spatial distributions. We now include an example of a two-dimensional map of HONO at 6 UTC time for the same representative day we used for NO_2. To our knowledge, this is the first time in which a 2D instrument is used to retrieve the HONO spatial distribution. The DSCDs simulated and calculated are in good agreement, and the comparison has a slope of 1.12 and a correlation coefficient of 0.99. In addition, the MAXDOAS-2D measurement of HONO has added value for air pollution research in the city since it is not measured by the in-situ monitors of the Council of Madrid air quality network. Therefore, our MAXDOAS-2D could provide some useful information regarding the mesoscale distribution of HONO, its role in the atmospheric chemistry in Madrid and its interactions with other trace gases such as NO_2.

Line 120: I am not sure that profile retrievals “try to reconstruct the photon paths” – in my view, they mainly try to find a vertical distribution that is consistent with the retrieved DSCDs

Thank you. We have changed this description for the sake of clarity and we have added a better RTM summary (from line 160 to line 163).

Table 1 / Table 2: I am not sure what exactly is meant by “All spectra and the Ring cross sections were allowed to shift and stretch (order 1) in wavelength”. However, in my opinion, reference spectra should not be allowed to shift and stretch as they are measured at high precision. If the background spectrum (here: the zenith-sky measurement) is well calibrated using a Fraunhofer Atlas, the only spectrum that should be allowed to shift and stretch is the horizon measurement itself.

Thank you for this comment. We think we failed to provide a clear explanation in our original submission. We only let to shift the measured spectra (with the MAXDOAS-2D) and the Ring, not the spectral absorption cross sections of the trace gases. We decided to include a shift to the Ring cross section because it is based on the inelastic rotational Raman scattering, which slightly changes the wavelength of the scattered photon when the scattering occurs, so it should have a little shift to improve the analysis. We checked the values of the Ring shift and although low, it improved the analysis, so we think that we could let the Ring shift in wavelength. This is now clarified in Tables 1 and 2.

Line 239: Cloud clearance using AERONET data will work in the direction of the sun, but as far as I know, it does not guarantee 360◦ of cloud free measurements.

We have added more information regarding the role of cloud measurements in our study. We mention the AERONET data because we compared the AERONET data with our MATLAB code data and the results are similar. Now, we have added the MATLAB code filter that we programmed from scratch (it is explained from line 312 to line 332).

Figure 4 and discussion: I did not fully understand what was done here and why -surely, it does not make sense to use an atmosphere for the wrong surface height. I also fail to understand what the conclusions i) and ii) exactly imply, and how they follow from the

fact that the profile retrieval is able to compensate a wrong atmospheric pressure profile by wrong extinction coefficients when reproducing O4 measurements.

We would like to take the opportunity to clarify that we did not use a wrong surface height, in which case we agree it would not make sense. We have used a height grid of layers that start right at the surface (0 m height). What we did was to interpolate the US Standard pressure profile (that is assumed to be accurate for the sea level) to the mean height of Madrid above sea level. Using those two sets of atmospheric profiles as examples, we ended up having very similar simulated DSCDs of O_4 in both cases, hence it seems that small variations in the atmospheric profiles do not affect significantly the O_4 analysis, thus we concluded in i) that the main driver of the O_4 retrieval are the measured O_4 DSCDs, which gives confidence to the overall analysis. However, each set of atmospheric profiles gave rise to notable differences in the extinction coefficients (especially above the surface layer). Therefore, we concluded that variations in physical parameters such as the pressure profile can produce changes in the extinction coefficients, hence given the difficulty to obtain very accurate atmospheric profiles, we think that as of now we cannot reliable assign those extinction values as particulate matter extinction (i.e. to aerosols). We prefer to discuss uncertainties in the atmospheric profiles rather than true or false profiles. Nonetheless, as shown in Figure 5, the fact that the simulated DSCDs still reproduce with high accuracy the measured O_4 DSCDs means that the light paths derived will be essentially the same (regardless the chosen atmospheric profile), and hence will ultimately generate almost the same results for the trace gases profiles.

Figure 9: I think it does not make sense to present two pieces of radial information from the onion peeling approach in this smoothed fashion that suggest a higher information content than there really is.

We tried to specify within the text that we carried out the calculations with two radial values, we decided to show the contour because we thought it would be easier to grasp both NO_2 location and its temporal variation at a glance. However, we understand the reviewer's point that interpolating from just two radial values may be misleading. Hence we have modified the figure in our revised manuscript to present our results through an usual polar plot without interpolation (see lines 638-641 for the figure caption).

Two-dimensional monitoring of air pollution in Madrid using a MAXDOAS-2D instrument

David Garcia-Nieto[1, 2], Nuria Benavent[1, 2], Rafael Borge[2] and Alfonso Saiz-Lopez[1]

[1] Department of Atmospheric Chemistry and Climate, Institute of Physical Chemistry Rocasolano, CSIC, Madrid 28006, Spain

[2] Universidad Politécnica de Madrid, UPM, 28006 Madrid, Spain

*Corresponding author: Alfonso Saiz-Lopez (a.saiz@csic.es)

Abstract

Trace gases play a key role in the chemistry of urban atmospheres. Therefore, knowledge about their spatial distribution is needed to fully characterize the air quality in urban areas. Using a new Multi-AXis Differential Optical Absorption Spectroscopy (MAXDOAS)-2D instrument, along with an inversion algorithm (bePRO), we report the first two-dimensional maps of nitrogen dioxide (NO_2) and nitrous acid (HONO) concentrations in the city of Madrid, Spain. Measurements were made during two months (May 6 -July 5 2019) and peak mixing ratios of 12 ppbv and 0.7 ppbv for NO_2 and HONO, respectively, were observed in the early morning in the south-pointing geometry. We found good general agreement between the MAXDOAS-2D mesoscale observations -which provide a typical spatial range of a few kilometers- and the in-situ measurements provided by Madrid´s air quality monitoring stations. In addition to vertical profiles, we studied the horizontal gradients of NO_2 in the surface layer by applying the different horizontal light path lengths in the two spectral regions included in the NO_2 spectral

analysis: ultraviolet (UV, at 360 nm) and visible (VIS, 477 nm). We also investigate the sensitivity of the instrument to infer vertically-distributed information on aerosol extinction coefficients and discuss possible future ways to improve the retrievals. The retrieval of two-dimensional distributions of trace gas concentrations reported here provides valuable spatial information for the study of air quality in the city of Madrid.

1 Introduction

Air pollution in urban areas has become a concern in our society because it represents a major risk to human health and the environment (WHO, 2019). Air quality is often expressed as the state of air pollution in terms of gaseous pollutant concentrations as well as size and number of particulate matter that may affect human health, ecosystems and climate (Monks et al., 2009). Integral understanding of air pollution requires knowledge about the sources, pollutants, chemical composition and spatial distribution, and their transport phenomena in the atmosphere (EEA, 2019).

Madrid, Spain, has suffered from severe air pollution in recent years, with episodes of large nitrogen dioxide (NO_2) and ozone (O_3) concentrations. In an effort to control and reduce high pollution events, the local government has enforced some traffic restriction measures (Izquierdo et al., 2020) and has set up several in-situ air quality monitoring stations over the city's metropolitan area. These in-situ instruments -as of today- cannot measure some important trace gases present in the atmosphere and their values are only representative of the immediate surrounding of the instruments and at surface level. There is therefore a need for mesoscale analysis (both in horizontal and vertical) of urban air pollution that could complement the in-situ measurements. With this aim, we have deployed

a Multi AXis Differential Optical Absorption Spectroscopy (MAXDOAS) instrument for air pollution measurements in Madrid. MAXDOAS is a widely used technique for the detection of trace gases in the atmosphere and it is based on the wavelength dependent absorption of scattered sunlight by atmospheric constituents (Platt and Stutz, 2008). In addition to routinely monitored, regulated species such as NO_2 and O_3, MAXDOAS provides mesoscale measurements of other trace gases that are relevant to understand atmospheric chemistry, such as nitrous acid (HONO), formaldehyde (HCHO) or glyoxal (CHOCHO). Over the past few years, we have reported trace gas measurements in Madrid using the MAXDOAS technique (Wang et al., 2016; Garcia-Nieto et al., 2018; Benavent et al., 2019) as well as pollutants trend analysis and chemical transport modelling (Borge et al., 2018; Cuevas et al., 2014; Saiz-Lopez et al., 2017).

For this work, a new two-dimensional MAXDOAS instrument (which will be described in Sect. 3 and will be hereafter referred to as MAXDOAS-2D) has been built, tested and set up to take continuous measurements in Madrid. This instrument represents a follow-up development to our previous one-dimensional instrument (MAXDOAS-1D, see Wang et al., 2016) that incorporates the capability of moving in the azimuthal dimension, therefore allowing the collection of spectra pointing at any angular direction. This additional capability allows the measurement of both the horizontal and vertical trace gas (e.g. NO_2) distribution throughout the city and in turn the generation of two-dimensional maps of trace gas concentrations. Several works using two-dimensional MAXDOAS instruments have been carried out in recent years (e.g. Ortega et al., 2015, Yang et al., 2019, Schreier et al., 2019, Dimitropolou et al., 2020). These studies were mostly focused on mapping the NO_2 distribution in urban environments and assessing its role for air quality monitoring.

Here we present two months of MAXDOAS-2D measurements of scattered sunlight spectra. The measurements were taken from May 6, 2019 to July 5, 2019, with focus on the evaluation of NO_2 vertical concentration profiles and the characterization of horizontal light path lengths. We will also provide the retrieval of HONO as an example of the potential of the MAXDOAS-2D measurements. This represents the first two-dimensional MAXDOAS measurements in Madrid. An assessment of the relation between the MAXDOAS analysis and the in-situ instruments in the city was carried out. Sect. 2 provides details of the DOAS technique while Sect. 3 describes the experimental setup. The inversion methods and the atmospheric parameters chosen for the analysis is detailed in Sect. 4. The two-dimensional NO_2 and HONO distributions, an evaluation of the light path geometries, along with their relative probabilities, and an assessment of horizontal mixing ratio gradients near the surface are discussed in Sect. 5. Finally, Sect. 6 contains conclusions and possible future work.

2 Brief introduction to the DOAS method

The absorption spectroscopy field has been developed for several decades within different research disciplines (such as remote sensing, astronomy or atomic and molecular physics). Its foundation relies on the absorption of radiation when interacting with a certain sample. The basic idea is described by the Beer-Lambert law, which models the exponential attenuation of spectral irradiance when it traverses a certain sample that contains some absorber species:

$$I(\lambda, L) = I_0(\lambda)\, exp\left(-\sum_i \int_0^L \sigma_i(\lambda)\, \rho_i(s) ds\right) \quad (1)$$

where λ is the radiation wavelength, σ_i and ρ_i stand for -respectively- the absorption cross section and concentration of a given absorber i along the path, while the pair I_0 and I represent the spectral irradiances at the beginning and end of the process at study. The absorption processes are integrated over the photon paths (with infinitesimal path ds) and summed over every present absorber (Platt and Stutz, 2008).

Specifically, the MAXDOAS technique is based on the study of the differential spectral absorption structures that are produced in the measured scattered sunlight spectra (Hönninger et al., 2004; Plane and Saiz-Lopez, 2006; Platt and Stutz, 2008). The main principle is based on identifying the narrowband absorption features within the measured optical density taking out the broadband optical density, mainly generated by Rayleigh and Mie scattering, as well as by instrumental effects. On the other hand, an analogous process is done on the trace gases absorption cross sections by means of filtering out the broadband spectral features, hence producing the so-called differential absorption cross sections, which are unique for each trace gas, acting as their "fingerprints" and therefore enabling their specific detection.

For MAXDOAS, I_θ stands for the solar spectrum (known as the Fraunhofer spectrum, with no Earth atmospheric absorptions), while I represents the recorded ground-based spectrum, which includes all the absorption and scattering processes. However, and since the actual photon path is difficult to determine with accuracy (see Sect. 4), the MAXDOAS calculations are done using relative absorptions between two different optical paths: a zenith spectrum -that contains less absorptions and is assumed as a reference spectrum- and other spectrum pointing to a given elevation angle. Therefore, the direct product of the method is the Differential Slant Column Density (DSCD), which can

be defined as the difference in the integrated concentration of a given absorber between the two selected pointing directions (more details about the numerical procedure that lies behind can be found in Honninger et al., 2004, Plane and Saiz-Lopez, 2006 and Platt and Stutz, 2008). Finally, these DSCDs are used as the main input for the profile retrieval algorithms, which simulate the state of the atmosphere with the purpose of reproducing the measured DSCDs. This final step yields the optimal vertical concentration profiles.

3 Experimental

Briefly, MAXDOAS-1D instruments consist of a light collector attached to a stepper motor that scans the atmosphere at different Viewing Elevation Angles (VEA, see Fig. 1). The main feature added to the MAXDOAS-2D instrument is an additional stepper motor for the azimuthal movement, hence allowing the light collector to freely point to any angular direction in the atmosphere. This allows the evaluation of trace gases absorptions for different Viewing Azimuth Angles (VAAs) (Fig. 1).

3.1 MAXDOAS-2D description

A new MAXDOAS-2D instrument (Fig. 2) was built by the Atmospheric Chemistry and Climate group at the Institute of Physical Chemistry Rocasolano (IQFRCSIC). Its main elements are based on our previous MAXDOAS-1D instrument: a light collector attached to a stepper motor, along with a focusing lens (80 mm focal length) are responsible for collecting the scattered sunlight. An Ocean Optics, SMA 905 optical fiber of 1-meter length conducts the light through an Ocean Optics, HR4000 spectrometer (which incorporates a linear silicon CCD array as detector). The spectrometer wavelength ranges roughly from 300 nm to

500 nm and offers an estimated spectral resolution (full width at half maximum) of about 0.5 nm. An additional stepper motor was included for azimuthal movement. The instrument incorporates all its components in an outdoor unit. Therefore, to maintain the spectrometer temperature as steady as possible -for both mechanical and wavelength calibration purposes- a Peltier cell was included. Additionally, an UPS device provides the power supply and eliminates possible strong power peaks. Two webcams take pictures of the cloud cover at each VAA, and monitor the instrument itself. The instrument is autonomous and it runs on a homemade Java software. This software controls the movement, the spectra collection and recording, the surrounding accessories and automatically keeps it continuously measuring as long as the Sun is over the horizon.

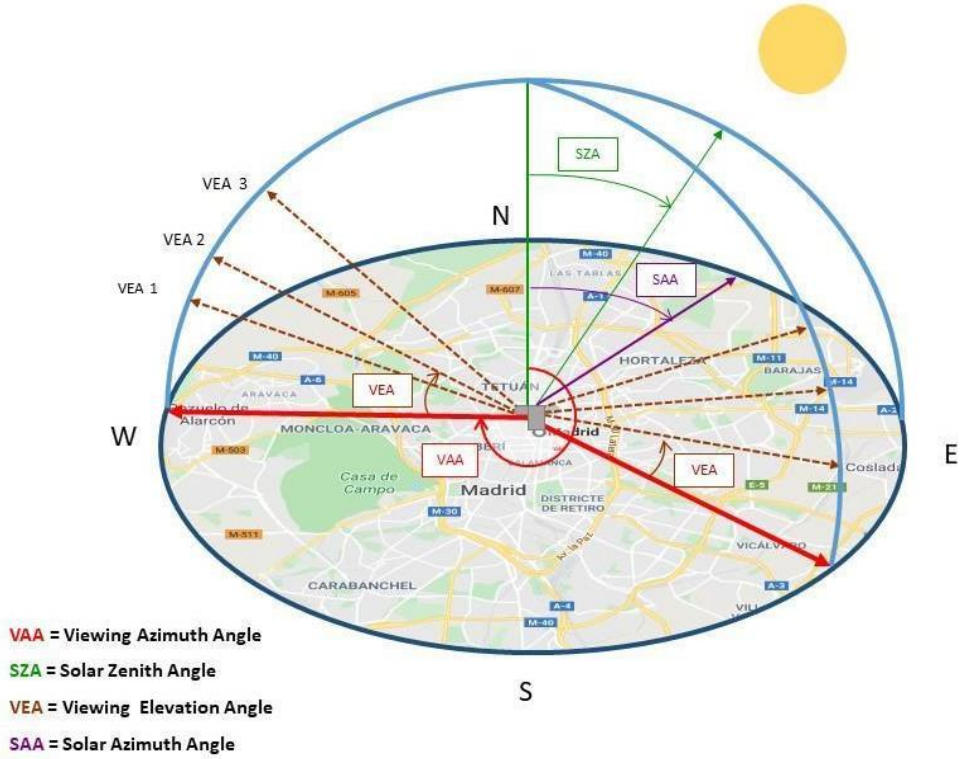

Figure 1. MAXDOAS-2D geometry diagram, the background of this picture represents the Madrid city center taken from Google Maps.

205 3.2 Location

206

207 The MAXDOAS-2D instrument is located at the main campus of the
208 Spanish National Research Council (CSIC) in Madrid, Spain. It is placed
209 on the roof of the Instituto de Ciencias Agrarias (ICA) at a latitude
210 of 40.4419° N and a longitude of 3.6875° W. The height of the building
211 is approximately 70 m above ground level. This location in downtown
212 Madrid can be classified as an urban site, with the usual weather of
213 continental areas at mid-latitudes (i.e. hot and dry summers and cold
214 winters), with prevalence of clear sky days during the year. NO_2
215 typically presents strong spatial concentration gradients in urban
216 areas and traffic hot-spots have been reported in Madrid (Borge et
217 al., 2016). This makes it difficult to clearly predict how NO_2 will be
218 distributed, i.e., there is not a clear azimuthal direction preference
219 for higher NO_2 at a certain time. However, mesoscale simulations
220 suggest that higher NO_2 mixing ratios can be expected in the southern
221 part of Madrid, considering population distribution and commuting
222 patterns (Picornell et al., 2019).

223

224 Due to some obstacles that blocked a clear view in some of the
225 VAAs, a small aluminum tower was built to overcome the viewing
226 obstacles and the MAXDOAS-2D instrument was fixed on top of it (see
227 Fig. 2). Once the instrument was set up, we aligned it for both angular
228 movements -azimuthal and zenithal- with respect to the geographical
229 north and the local horizontal (i.e. perpendicular to the gravitational
230 plumb), respectively. This process was performed in two steps: first,
231 the light collector was coarsely oriented using levels and a compass.
232 Then, the alignment was refined doing a vertical scan of the Sun (which
233 has a very well-known position vector) and its angular surroundings
234 at several different times of a clear sky day. The angular differences
235 between the measurements and the center of intensity of the registered

spectra (a similar approach was done in Ortega et al., 2015) were estimated and the associated correction applied to the instrument.

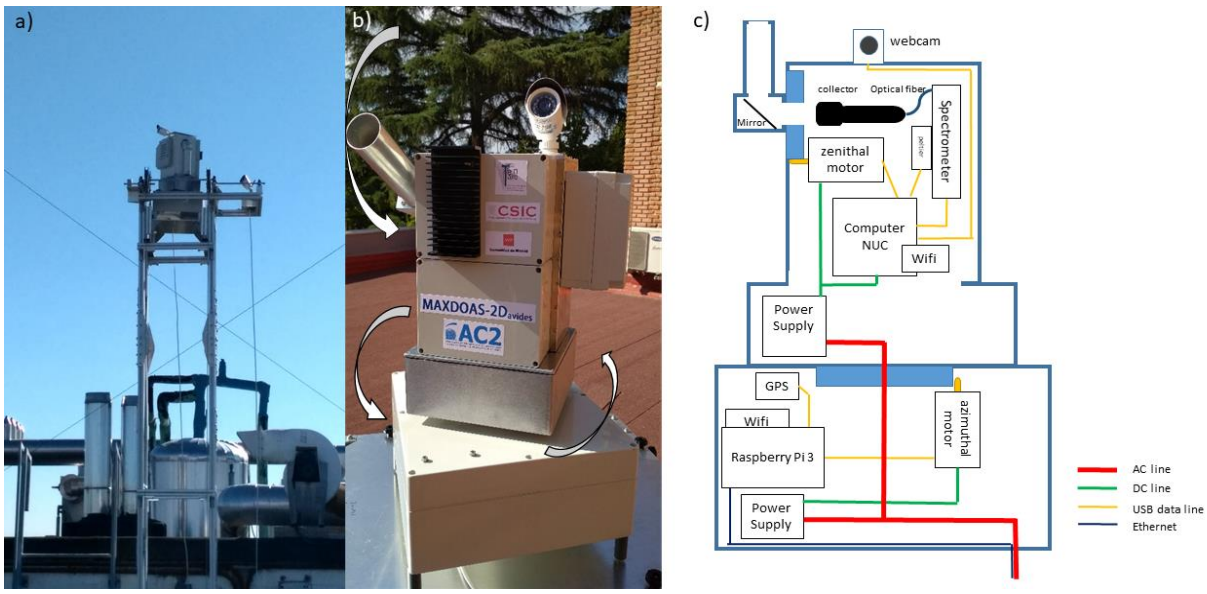

Figure 2. a) Aluminum tower with the instrument installed on top of it; b) MAXDOAS-2D instrument; c) MAXDOAS-2D scheme.

3.3 Measurements set up

In order to sample and analyze a representative portion of the atmosphere over Madrid, selected angular directions were chosen. Starting at a VAA of 0º (pointing to the north), the MAXDOAS-2D rotated clockwise using steps of 20º in azimuth. In each azimuth direction, the ensuing VEA vector was used: 1, 2, 3, 5, 10, 30 and 90 degrees. Therefore, an entire azimuthal lap was completed when the light collector was back again at VAA of 0 degrees.

For every measured spectrum, the spectrometer was able to correct for both electronic offset and dark current effects. Other important parameters for the measurements such as the integration time and the

number of scans taken in each angular direction were automatically calculated by the software. More specifically, for this study we set the goal of completing an azimuthal lap in approximately one hour (mainly for an easier interpretation of the results and for the subsequent comparison with in-situ instruments of Madrid´s air quality monitoring network). Hence, we chose 24 seconds as the maximum exposure time in each angular combination.

The main advantage of this set-up is that we can observe the daily NO_2 variability over the entire city with a moderate temporal resolution (1-hour). The main disadvantage is that observations for each VAAs averaged over such a short integration period may be affected by microscale phenomena. Nonetheless, NO_2 concentration gradients are particularly strong in space (Borge et al., 2016). Therefore, this exposure time may be well suited to characterize both the azimuthal and the horizontal gradients of NO_2.

4 Analysis methods

Using the DOAS technique, the absorptions of the molecular oxygen dimer (O_4) and NO_2 were measured for the entire campaign and for two spectral windows: 352-387 nm (UV region) and 438-487 nm (VIS region). The analysis settings applied for the UV and VIS regions are summarized in Tables 1 and 2, respectively. These configurations follow those used in Wagner et al., 2019.

Table 1. DOAS spectral settings for the retrieval of O_4 and NO_2 in the UV.

Parameter	Value

Fitting window	352-387 nm
Wavelength calibration	Based on reference solar atlas (Chance and Kurucz, 2010)
Zenith reference	Scan
Polynomial Order	5
Intensity Offset	Order 2
Shift	The measured spectra and Ring were allowed to shift and stretch (order 1) in wavelength.

Molecule	Cross section
O_4	293 K (Thalman and Volkamer, 2013)
NO_2	298 K (Vandaele et al., 1998)
O_3 a	223 K (Serdyuchenko et al., 2014)
O_3 b	223 K (Serdyuchenko et al., 2014)
HCHO	297 K (Meller and Moortgat, 2000)
HONO	296 K (Stutz et al., 2000)
Ring_a	Calculated by QDOAS
Ring_b	Ring_a spectrum multiplied by λ^{-4}

285 Table 2. DOAS spectral settings for the retrieval of O_4 and NO_2 in the
286 VIS.

Parameter	Value
Fitting window	438-487 nm
Wavelength calibration	Based on reference solar atlas (Chance and Kurucz, 2010)
Zenith reference	Scan
Polynomial order	5
Intensity offset	Order 2
Shift	The measured spectra and Ring were allowed to shift and stretch (order 1) in wavelength.
Molecule	**Cross section**
O_4	293 K (Thalman and Volkamer, 2013)
NO_2	298 K (Vandaele et al., 1998)
O_3 a	223 K (Serdyuchenko et al., 2014)
O_3 b	223 K (Serdyuchenko et al., 2014)
H_2O	296 K (Rothman et al., 2010)
Glyoxal	296 K (Volkamer et al., 2005)
Ring a	Calculated by QDOAS
Ring b	Ring a spectrum multiplied by λ^{-4}

287

The selected differential absorption cross sections -along with the spectral window and parameters included in Tables 1 and 2- were adjusted to the measured differential optical density using the QDOAS spectral fitting software (developed at BIRA-IASB, http://uv-vis.aeronomie.be/software/QDOAS/). When the measured DSCD (using QDOAS) accurately matches the differential optical density for a given trace gas -i.e. yielding a relatively low residual- there is positive detection of that trace gas. Figure 3 shows examples of spectral detection of O_4 and NO_2 for both the UV and VIS regions. Once the DSCDs are obtained, they are used as input for the profile retrieval algorithm, as explained in Sect. 4.2.

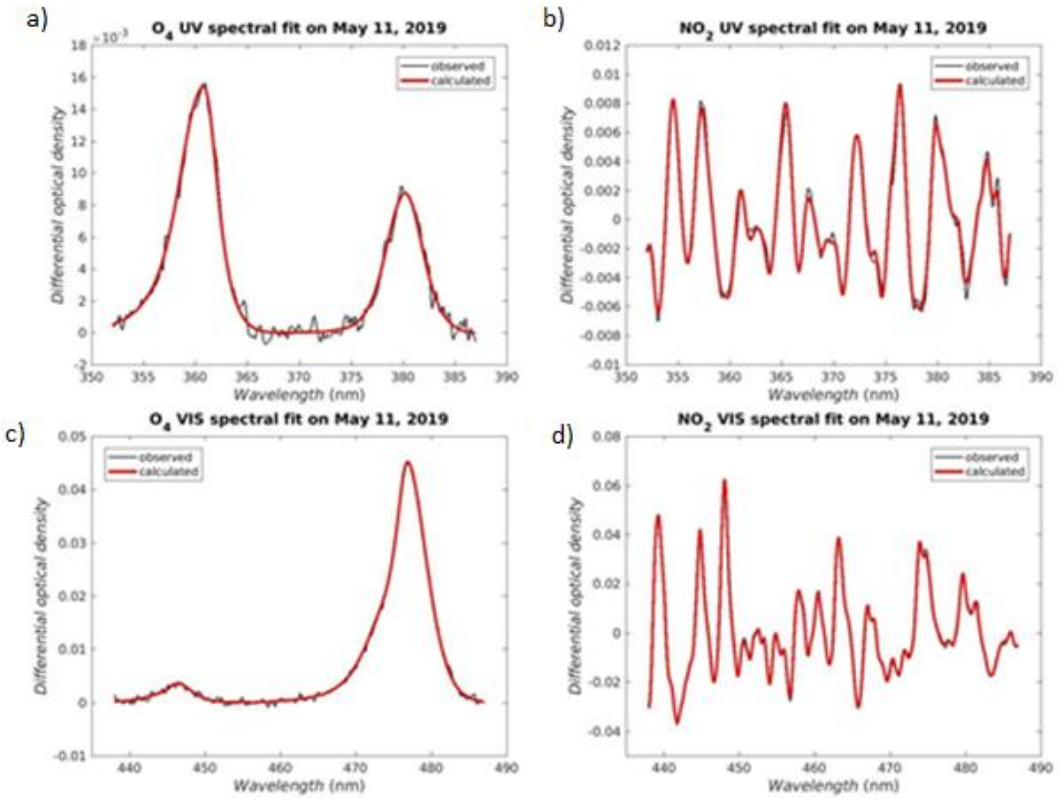

Figure 3. Spectral detection of O_4 (a) and (c) and NO_2 (b) and (d), red lines represent the calculated optical densities and black lines are the measured optical densities.

4.1 Cloud-screening and quality filtering

306

307 The algorithms for MAXDOAS retrievals of trace gas vertical
308 profiles are based on estimating the light paths (along with their
309 corresponding scattering probability) for a clear sky day. A
310 significant cloud cover could noticeably impact the calculations,
311 mainly because of multiple scattering effects, adding large
312 uncertainties to the retrieval process. For this reason, the set of
313 measured spectra has to be cloud-screened, filtering out those spectra
314 affected by clouds. In order to achieve that, we used the cloud-free
315 AERosol RObotic NETwork (AERONET) database. AERONET is a global network
316 of ground-based remote sensing instruments established by NASA and
317 PHOTONS (https://aeronet.gsfc.nasa.gov/new_web/index.html) to measure
318 aerosols and their optical, microphysical and radiative properties.
319 The AERONET instruments provide a long-term, continuous and readily
320 accessible public domain database of aerosol measurements worldwide.
321 These databases are reported with three quality levels, in particular,
322 we used the Level 2.0 (cloud-screened and quality-assured) database
323 provided by the AERONET instrument placed in Madrid. This information
324 is combined with the photos taken by the camera installed on the
325 MAXDOAS. As mentioned in Sect. 3.1, this webcam points at the same
326 azimuthal direction as the light collector, therefore we had a set of
327 azimuthal photos of the sky for each horizontal lap. We estimated the
328 cloud cover using a code that gets the RGB coordinates -the three
329 chromatists of the blue, green and red- and it changes them into LCh
330 coordinates -L indicates lightness, C represents chroma and h is the
331 hue angle. Based on criteria of luminosity, colour and saturation, the
332 code estimates the cloud index.

333

334 Since we are dealing with a non-linear, least-squares system of
335 equations, there is a notable gradient concerning the quality and
336 uncertainties in the results. Hence, before proceeding with the
337 profiling algorithm, several quality filters were applied to the DSCDs:
338 firstly, every DSCD that yielded either a relative uncertainty larger

than 1 or a residual Root Mean Square (RMS) higher than 0.01 (in optical density units) was rejected. After that, we estimated the DSCDs detection limit for a given trace gas as the ratio of the residual RMS (in optical density units) associated to each DSCD and the maximum value of the differential cross section of that trace gas. Then, we discarded the DSCDs that had an absolute value lower than twice the derived detection limit (a similar approach was carried out in Peters et al., 2012). Finally, we used the daily plus/minus three standard deviation criterion that AERONET applies for its cloud-filtered data, keeping the DSCD that falls within plus/minus three standard deviations from each daily mean. Overall, the number of MAXDOAS DSCDs cycles that were considered valid after the quality checks was slightly above 90 % for both trace gases and spectral regions.

4.2 Inversion algorithm and vertical profiles

We applied an inversion algorithm method to the measured DSCDs to estimate the light paths and subsequently derive the trace gas vertical concentration profile. The main idea behind these inversion algorithms is based on the fact that each VEA has different scattering heights and light paths (Solomon et al., 1987). Therefore, a given set of measured DSCDs contains information about the vertical distribution of a certain trace gas. Since higher VEAs are generally related to higher scattering heights, different layers within the atmosphere can be sampled, especially in the lower troposphere. The forward models that calculate these scattering events are called Radiative Transfer Models (RTMs), and they study the transport of radiation as well as its interaction with matter. Each inversion algorithm needs a forward model that simulates the atmosphere in order to estimate the light paths and retrieve the vertical profiles of trace gases. There are several inversion algorithms for atmospheric applications, but for

this work we have used the bePRO inversion algorithm, developed at BIRA-IASB (Clémer et al., 2010). The original calculation was built based on the Optimal Estimation Method (OEM; Rodgers, 2000) and it comprises two steps: first, the light paths and the vertical profiles of irradiance extinction are calculated using the O_4 DSCDs; then, the target trace gas vertical concentration profile is retrieved using the corresponding light paths and measured absorption. In order to do that, bePRO simulates the atmospheric state characterizing several different physical phenomena including pressure and temperature vertical profiles, Rayleigh and Mie scattering events (along with their respective phase functions), the effect of the surface albedo, the light path geometries or the irradiance extinction processes. Once the atmospheric vector state is defined, its combination with a certain vertical concentration profile results in the simulated DSCDs. This vertical profile is iterated until the generated set of simulated DSCDs is optimized with respect to the measured DSCDs so that the residual is minimized. As a result, an optimal vertical profile is obtained when the iteration is finished for each MAXDOAS cycle.

The measured O_4 DSCDs are used to estimate the light paths for each VEA since they are related to the square of the atmospheric O_2 profiles, which are well-known. This profile is fairly steady during the day and does not heavily depend on chemistry factors. Therefore, the measured O_4 DSCDs can provide information on the irradiance extinction in the atmosphere. This extinction profile is usually associated with the aerosol extinction coefficients and thus, its vertical integration yields the Aerosol Optical Depth (AOD). These aerosol extinction profiles are required to subsequently evaluate trace gas profiles since they strongly affect the relative light paths and hence the concentration profiles derived from them.

Once the light paths are computed in the previous step, and with the purpose of best simulating the measured DSCDs, a linear analysis process is performed for the measured DSCDs of the target trace gas, yielding the optimal vertical concentration profile. The vertical integration of this concentration profile is called the Vertical Column Density (VCD).

The retrieval consists of an iterative, nonlinear system of equations, and hence there is no unique solution. This means that an a priori profile is needed, both for starting the iterations and to avoid the final solution to be non-realistic (i.e. with no physical meaning). In order to construct these a priori profiles we used exponentially decreasing curves as follows:

$$ap\,(z) = \frac{VC_i}{sh} exp\left(\frac{-z}{sh}\right) \quad (2)$$

where $ap\,(z)$ is the a priori vertical profile at a certain altitude z, VC_i is the vertical integration of the profile for the MAXDOAS cycle i and sh is the scaling height constant. We used 0.5 km as the scaling height constant for all the a priori profiles (Hendrick et al., 2014). Regarding the VC, we assumed an AOD of 0.05 for the O_4 retrieval, while for NO_2 we applied the geometrical approximation followed in Hönninger et al., 2004, taking the measured DSCD at VEA 30º for every MAXDOAS cycle. This approximation assumes that most of the absorption events are located below the scattering height.

With respect to the remaining atmospheric parameters, we chose typical values for urban environments: surface albedo of 0.07, correlation length of 0.4 km and an a priori covariance factor of 1 (see Hendrick et al., 2014). We use the air number density vertical

profile since it is directly related to the number of O_4 absorptions, and therefore to the O_4 DSCDs. Hence the relative differences, particularly for lower VEAs, between the measured and simulated O_4 DSCDs are usually assigned to aerosol extinction. Note however, as shown below, that uncertainties in the air number density profiles - arising from uncertainties in the values or shape of the temperature and pressure profiles- could also explain such differences (Fig. 4).

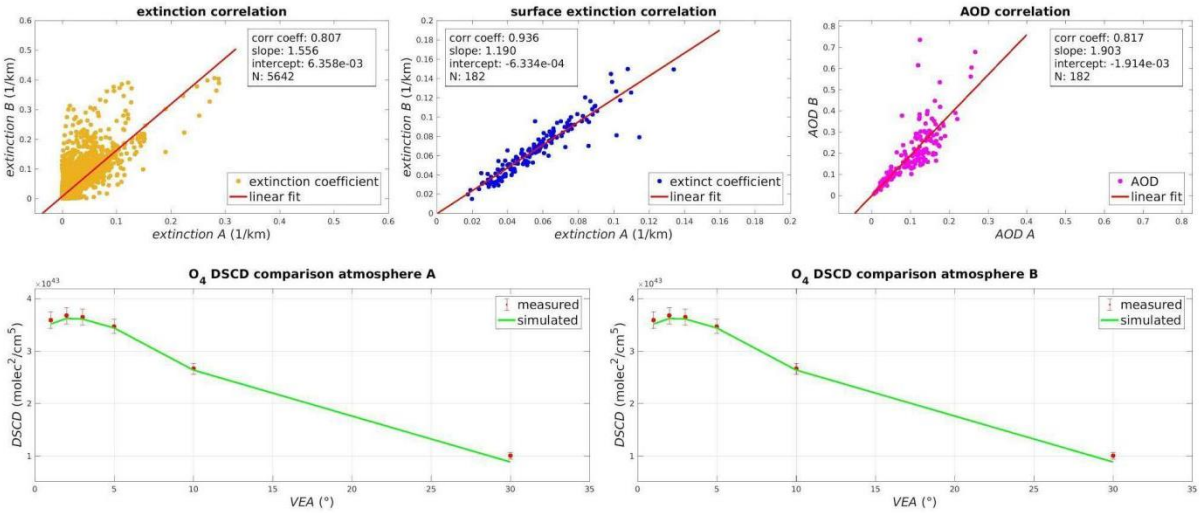

Figure 4. Comparison of retrieved aerosols using two different atmospheric profiles: the US Standard (atmosphere A) and the US Standard adapted to the altitude above sea level of Madrid (atmosphere B).

Here we compare the simulation of O_4 DSCDs using two different sets of atmospheric profiles: i) the US Standard, and ii) the same profile but interpolating the pressure profile to Madrid´s height above sea level (mean value of 667 m). This means that the temperature profile is assumed to be the same but the pressure profile is shifted less than 10%, so there are no major variations within the profiles. The lower row in Fig. 4 shows that both atmospheric profiles result in almost the same set of simulated O_4 DSCDs, however the aerosol

extinction coefficients differ significantly (although less for the surface layer coefficients), and consequently, the AOD also varies. From this we infer that:

i) the retrieval is mainly driven by the measured DSCDs, which leaves a relatively low weight for the chosen atmospheric profiles (pressure and temperature). Therefore, we can obtain consistent correlations between the measured and simulated O_4 DSCDs.

ii) we cannot reliably assign the extinction coefficients at each layer to aerosols (especially for atmospheric layers above the surface layer), but rather consider them as irradiance extinction coefficients.

Furthermore, we have assessed the impact of the pressure and temperature profiles choice on the trace gas retrieval. As can be noted in Fig. 5, there is no significant effect coming from this choice on the simulated NO_2 DSCDs. These are basically the same (and with very good agreement with the measured DSCDs), as well as the derived concentration coefficients and their integration (VCD).

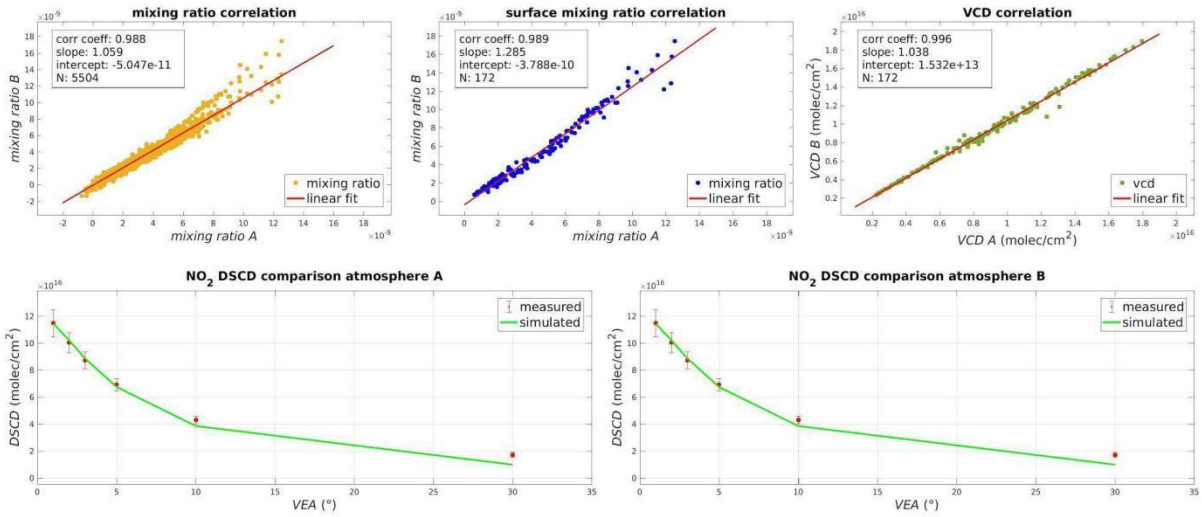

Figure 5. NO_2 retrieval comparison using two different atmospheric profiles: the US Standard (atmosphere A) and the US Standard adapted to the altitude above sea level of Madrid (atmosphere B).

However, we also evaluate if a similar behavior can be expected for larger variations in the pressure and temperature profiles. We first obtained the average surface temperature and pressure values for the duration of the campaign (May-July, 2019). With the inclusion of these values in the retrieval, we found that, within the first 10 km height, the RMS of the relative variations with respect to the standard atmosphere were about 8 %. Although it is a small change, it is indeed not negligible. Nonetheless, when evaluating light paths, the relative changes were below 2%. Therefore, here we use the US Standard atmospheric profiles for the NO_2 retrievals.

Table 3 summarizes the average uncertainties (using one standard deviation for each component) of the retrieval, along with their relative contributions, for the ground layer (0-200 m height). he mean, overall uncertainty for NO_2 in both spectral regions is in the order of 10%.

Table 3. Summary of average uncertainties of the retrieval in both spectral regions.

Variable \ Trace gas	NO_2 UV (%)	NO_2 VIS (%)
Irradiance Extinction	7.7	5.1
DSCD	4.8	3.2
Surface Mixing Ratio	5.0	8.7
Total	10	11

4.3 Estimation of NO_2 horizontal gradients

Making use of the different paths that photons travel through the atmosphere for different wavelengths, we can estimate the horizontal distribution of NO_2. We use the estimated horizontal light paths at two wavelengths, 360.8 nm and 477 nm, for the surface layer (0-200 m height). The different light paths at 360.8 and 477 nm provide information about the horizontal distribution of NO_2 mixing ratios within the surface layer. In order to evaluate these horizontal paths, we have used our own codes that implement the RTM equations based on previous pioneering work (Solomon et al., 1987). These equations yield a vector of scattering events along with their respective probabilities. If we take a VEA of 0 degrees (i.e. horizontal viewing), then the scalar product of such vectors produces the length of the horizontal light path. We computed this for every MAXDOAS cycle and for both wavelengths, yielding typical -representative- horizontal distances of about 8-10 km for the UV (at 360.8 nm) and between 15-20 km for the VIS window (at 477 nm). The next step follows the “onion-peeling” approach proposed by Ortega et al. 2015 (the strong dependence of scattering with wavelength means that shorter wavelengths result in shorter light paths). We assign the UV (i.e. 360.8 nm) mixing ratios

(mr_{uv}) and their expected horizontal paths (d_{uv}) to the first peel (mr_A, meaning zone A). Then the second peel (zone B, mr_B) can be derived as:

$$mr_B = \frac{mr_{vis} \times d_{vis} - mr_{uv} \times d_{uv}}{d_{vis}} \quad (3)$$

Thereby, deriving mixing ratios (mr_a and mr_b) representative of two different horizontal distances for each VAA.

5 Results

5.1 O_4 and NO_2 DSCDs assessment

Once the vertical profiles are retrieved using the RTM explained in Sect. 4, we compare the set of simulated DSCDs predicted by the model with the measured DSCDs coming from the absorption analysis. An estimation of the overall goodness of the profile retrieval comes from the correlation between the measured and simulated DSCDs for the entire campaign (Fig. 6).

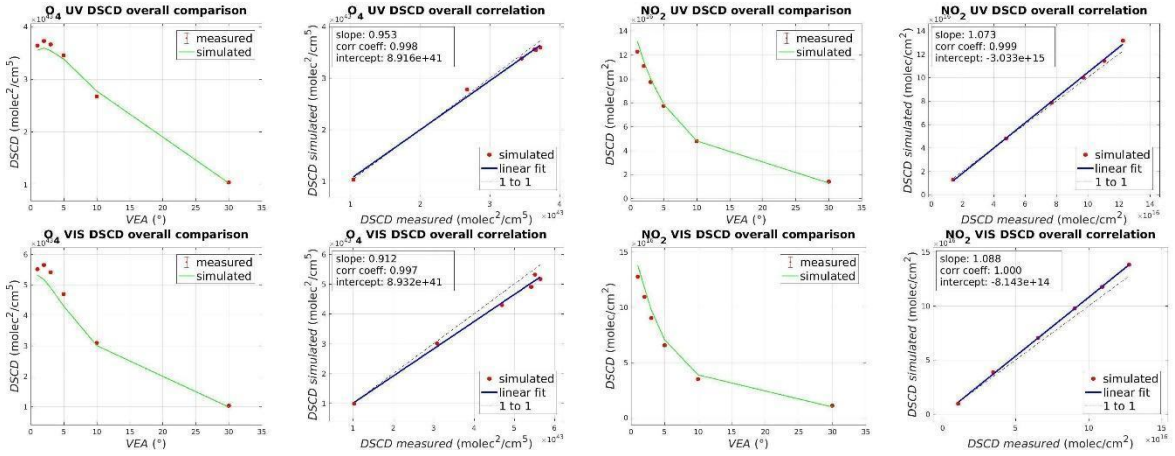

Figure 6. Comparison between simulated and measured DSCDs of O_4 and NO_2.

The fit between the measured and the simulated DSCDs shows correlations (r^2) very close to 1 for both O_4 and NO_2 in the UV and VIS regions. As mentioned before, the inverse retrieval finds the optimal solution of the vertical concentration profile that generates the best set of simulated DSCDs.

5.2 Two-dimensional maps

We now combine the VAA and height for each azimuthal cycle of the MAXDOAS-2D to generate a two-dimensional concentration map. Fig. 7 shows an example of the O_4 retrieval in the UV for a given azimuthal cycle. In addition to the profiles, Fig. 7 also shows the comparison and correlation of measured and simulated DSCDs for that azimuthal cycle, along with the evolution of retrieved AOD. The AOD varies between 0.05 and 0.18 within this azimuthal cycle (Fig. 7, upper panel). The contour plot shows the irradiance extinction coefficient profiles with maximum values of 0.14 km^{-1} (near the ground and at around 40º VAA) associated with aerosol extinction (see discussion in Sect. 4.2). Note the enhanced extinction at about 2 km height pointing at 50 VAA. This could be due to particulate matter emitted by traffic (there is a main road at that location) (Carnerero et al., 2018). Further research is needed to better establish the vertical distribution of aerosols in Madrid, and their diurnal evolution.

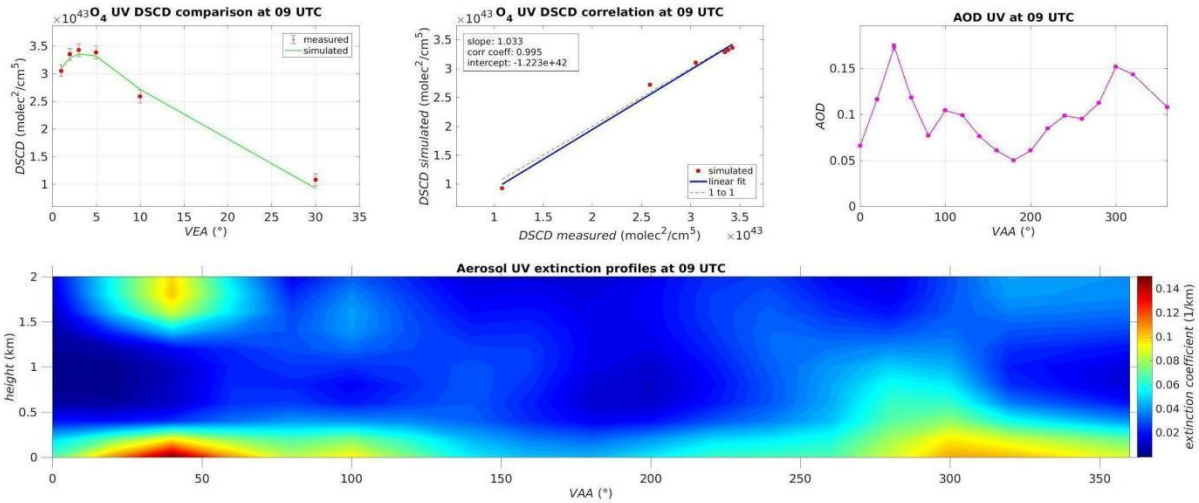

571

572 Figure 7. Example of O_4 and AOD retrievals in the UV region at 9
573 UTC on May 11, 2019. These contour plots are smoothed from adjacent
574 VAA data points separated by 20º in order to estimate the azimuthal
575 distribution of the irradiance extinction coefficients over Madrid.

576

577 Figure 8 presents a two-dimensional representation of NO_2 on May
578 11, 2019 at two different hours (6 UTC and 12 UTC, respectively). Both
579 contour plots show maximum NO_2 values of 12 ppbv at 6 UTC and 8 ppbv
580 at 12 UTC, when the instrument is pointing south (i.e. VAA of 180º).
581 We chose to show this day as an example since it was a clear sky day
582 and yielded NO_2 mixing ratios that were representative of the entire
583 period of measurements. These values correspond to the layer near the
584 ground and are in good agreement with our previous MAXDOAS observations
585 in Madrid (Garcia-Nieto et al., 2018). The retrieved azimuthal
586 distribution of NO_2 agrees with previous reports that show higher
587 pollution levels in the southern section of Madrid (Picornell et al.,
588 2019). NO_2 VCDs range from $5x10^{15}$ molecules cm^{-2} (at 12 UTC and pointing
589 at 300 º VAA) up to $15x10^{15}$ molecules cm^{-2} (at 12 UTC and pointing at
590 200º VAA), with an average value of $1x10^{16}$ molecules cm^{-2}. Although
591 there can be different NO_X emission rates at both times of the day (6
592 and 12 UTC), the increase in the boundary layer height during the day
593 could explain the similar values of VCDs at both hours but generally
594 lower surface mixing ratios at 12 UTC. Note that NO_2 is efficiently

mixed within the boundary layer as it develops during the day (i.e. boundary layer height usually lags the solar zenith angle) (Fig. 8) (de la Paz et al., 2016).

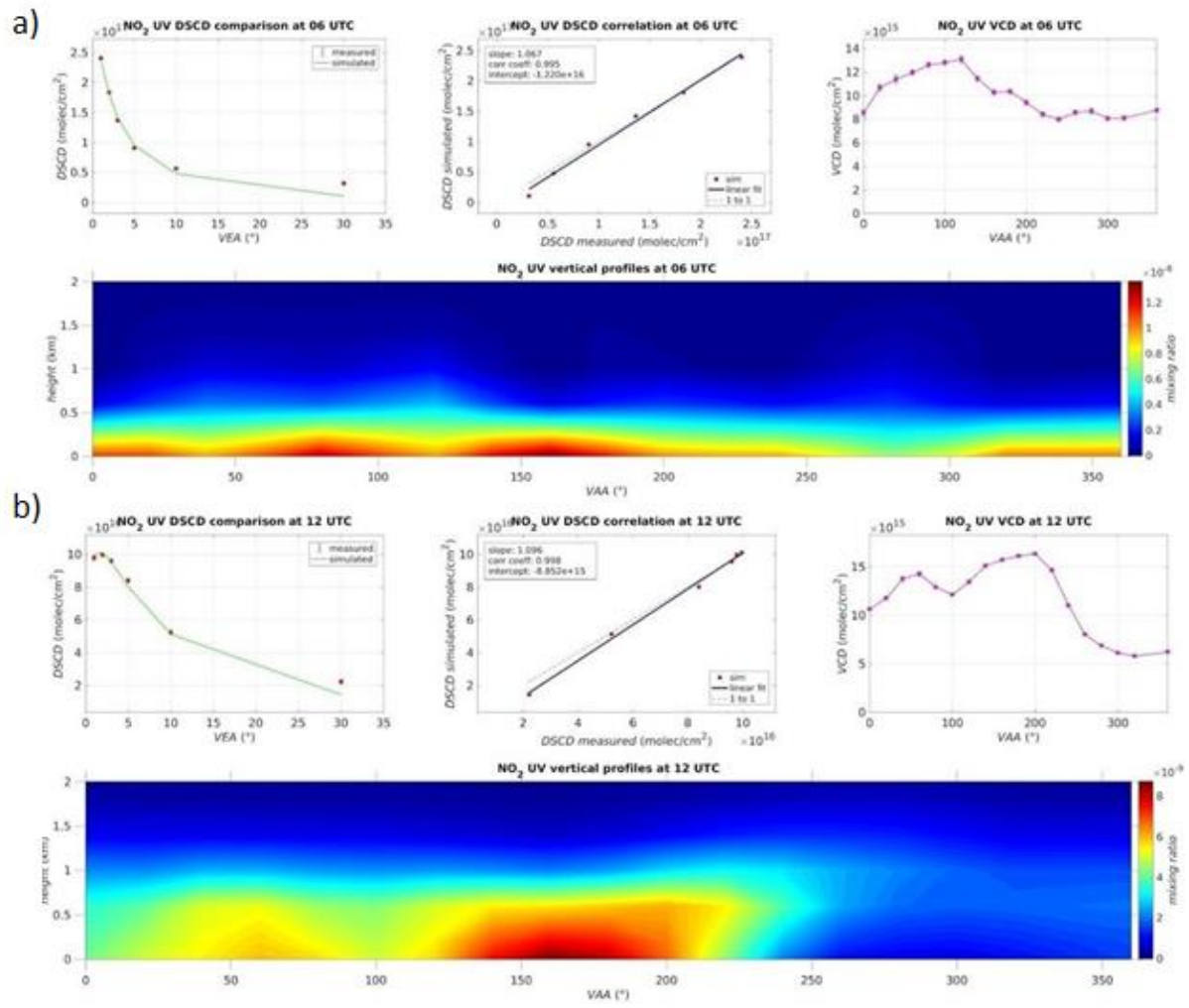

Figure 8. NO_2 vertical distribution retrieved in the UV region at 6 UTC (a) and at 12 UTC (b) on May 11, 2019. These contour plots are smoothed from adjacent VAA data points separated by 20º in order to estimate the azimuthal distribution of NO_2 over Madrid.

We have also analyzed HONO DSCDs measured by the MAXDOAS-2D using the same configuration as in Garcia-Nieto et. al., 2018. Figure 9 shows a two-dimensional representation of HONO on May 11, 2019 at 6 UTC. We retrieve surface layer peak values of 0.7 ppbv pointing at 50°

of VAA in the early morning, in agreement with previous studies for HONO in urban environments (see Hendrick et al., 2014; Ryan et al., 2018). The VCDs at 6 UTC range from $6x10^{14}$ to $1.2x10^{15}$ molecule cm^{-2}. The combination of spatially distributed measurements of NO_2 and HONO can be used together with chemical transport models to further understand pollution dynamics in Madrid.

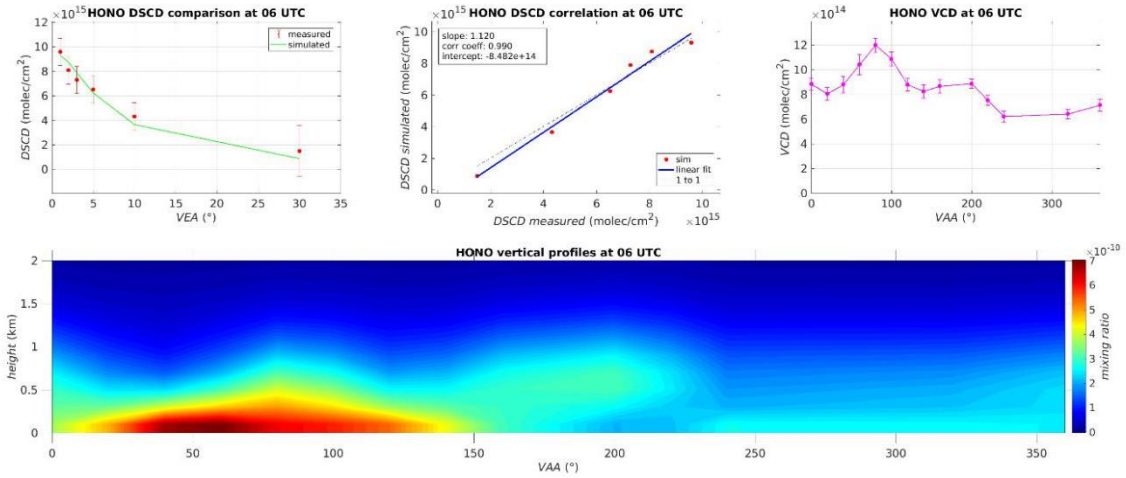

Figure 9. HONO vertical distribution retrieved in the UV region at 6 UTC. These contour plots are smoothed from adjacent VAA data points separated by 20º in order to estimate the azimuthal distribution of HONO over Madrid.

5.3 Horizontal distribution of NO_2

Based on Eq. (3), we derive the horizontal distribution of NO_2 in the surface layer (0-200 m height). Figure 10 shows an example of surface layer NO_2 mixing ratios over two radial distances from the MAXDOAS-2D instrument (using the UV and the VIS NO_2, respectively, as explained in Section 4.3), located at the center of the plot. The highest mixing ratios occur during the first sunlit hours (7-8 UTC), coincident with the morning peak of NO_X emissions in Madrid (Quassdorff et al., 2016). This early morning peak is followed by a gradual

632 decrease in surface layer NO_2 mixing ratios during the day. Note that
633 NO_2 is predominantly located in the southern part of the semisphere
634 (VAA from 90º to 270º).

635

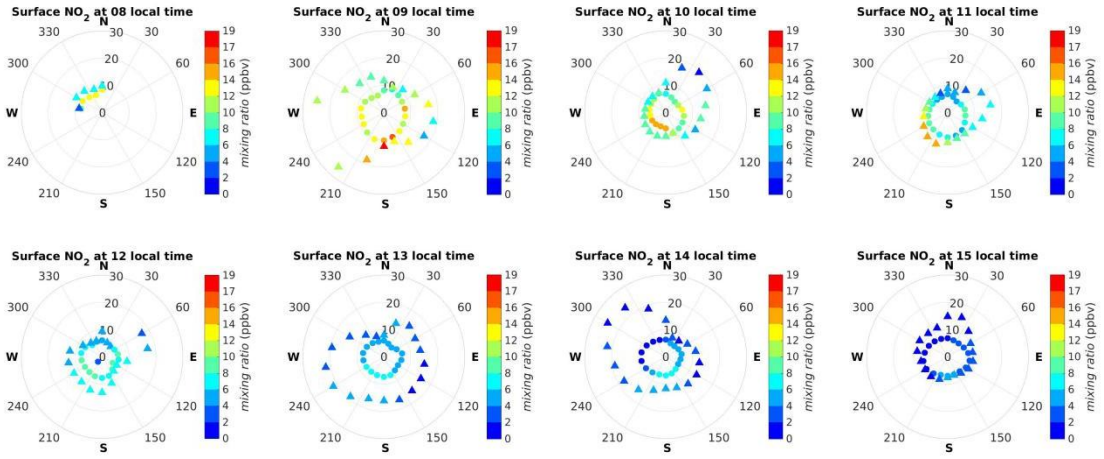

636

637 Figure 10. Polar plots of NO_2 within the surface layer (0-200 m height)
638 for May 11, 2019. Please note that these polar plots extend over a
639 direction perpendicular to those shown in Fig. 8. Here, circles are
640 used for the UV (shorter horizontal light path) and triangles for the
641 VIS (larger horizontal light path).

642

643 5.4 Correlation with Madrid´s in-situ air quality monitoring stations

644

645 We suggest that MAXDOAS-2D mesoscale observations may complement
646 the information provided by the local air quality monitoring network
647 based on reference analytical techniques (according to Directive
648 2008/50/EC). While air quality monitors of the reference network
649 provide information about ambient concentrations in their specific
650 locations (currently 24 air quality monitoring stations measure NO_2
651 within the city, see AM, 2019), MAXDOAS-2D observations produce near
652 ground-level concentrations averaged over the optical path in a given
653 direction. That prevents us from quantitatively comparing both types

of observations. Nonetheless, we analyzed their correspondence using the NO_2 concentrations measured by the in-situ instruments throughout the entire city, and the NO_2 mixing ratios within the surface layer derived from our MAXDOAS-2D instrument over the 2-month period (May-June, 2019). For this comparison, we considered the air quality monitoring stations within a distance from the MAXDOAS-2D equal or lower than 10 km. Since this is the typical horizontal light path for the UV region, we decided to include only the NO_2 values retrieved in the UV region for the comparison. Strong gradients between the values measured by the in-situ instruments are typical. Therefore, and considering that we are mainly interested in their temporal correlation with respect to our MAXDOAS-2D measurements, we compare both the in-situ NO_2 and surface layer MAXDOAS-2D hourly-averaged data. Note that for the MAXDOAS-2D this approximately corresponds to averaging the surface layer values for each azimuthal lap, given that each azimuthal lap takes approximately 1 hour to complete.

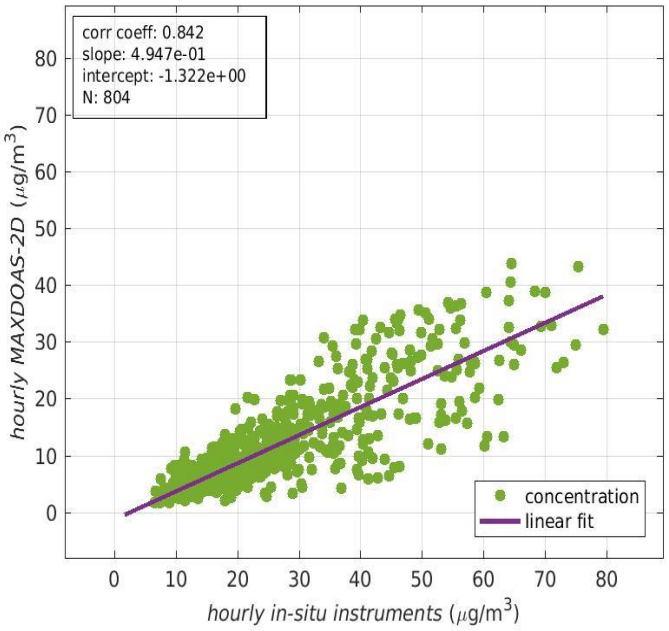

Figure 11. Correlation between in-situ observations from Madrid´s air quality monitoring network and those derived from the MAXDOAS-2D

674 instrument for the surface layer (0-200 m height).

675

676 Despite the different spatial representativeness, Figure 11 shows
677 a reasonably good correlation coefficient of 0.842 between both
678 datasets for the two-month campaign. The slope is lower than 1, this
679 can be explained by the typical NO_2 vertical profiles in urban
680 environments. Simulations performed over Madrid with a high-resolution
681 Eulerian air quality model (Borge et al., 2018) yielded an
682 exponentially decreasing with height NO_2 profile. Therefore, the
683 MAXDOAS-2D mixing ratios, which represent an average across the surface
684 layer (0-200 m height), are not expected to quantitatively match the
685 values of in-situ instruments, located close to the surface (between
686 0-10 m height). Similar conclusions -and slopes comparable to the one
687 retrieved above- regarding the correlation between in-situ and MAXDOAS
688 instruments can be found in previous works (Schreier et al., 2019;
689 Kramer et al., 2008; Chan et al., 2020). In addition, there is a good
690 temporal correlation between in-situ and MAXDOAS-2D measurements over
691 an extended period of time.

692

693 ## 6 Summary and Conclusions

694

695 An analysis of O_4, NO_2 and HONO vertical concentration profiles
696 in the urban atmosphere of Madrid (Spain) has been performed over two
697 months (from May 6 to July 5, 2019). We analyzed the absorptions and
698 derived the corresponding DSCDs for both trace gases in the UV and VIS
699 regions. Then, the corresponding profiles were retrieved using a RTM.
700 In this step, we assessed the impact of different atmospheric profiles
701 (pressure and temperature) in the retrieval results, and found that
702 the set of chosen atmospheric profiles has a small impact on the O_4
703 retrieval and the estimation of light paths. However, there is a
704 noticeable change in the irradiance extinction profiles, which makes

difficult to quantitatively assign extinction due to aerosols, especially in heights above the boundary layer.

The overall comparison of measured and simulated trace gas DSCDs showed that they were in very good agreement (with correlation coefficients close to 1), supporting the reliability of the observations. The MAXDOAS-2D instrument provides the first two-dimensional view (in height and VAA) of pollution concentration in the city of Madrid. Exploring one day (May 11, 2019) we compared two hours: the peak rush hour and noon time, obtaining NO_2 maximum values of 12 ppbv and 8 ppbv respectively, both maxima pointing to the south direction. Two-dimensional HONO measurements were also made with mixing ratio peaks of 0.7 ppbv in the early morning, and VCDs ranging from $6x10^{14}$ to $1.2x10^{15}$ molecule cm^{-2}.

We have also inferred information on the horizontal gradient of NO_2 within the surface layer making use of the strong dependence between wavelengths and light paths across the NO_2 absorption spectrum. The resulting "onion-peeling" figures indicate peak values of NO_2 in the early morning and in the southern section of the city (around 180 º VAA), it resulted in a gradual decrease in NO_2 mixing ratios during the day, maximum values of NO_2 appear in the southern part of the semisphere. Finally, we suggest that the new mesoscale information provided by the MAXDOAS-2D instrument helps in the study of pollution transport dynamics. MAXDOAS-2D and in-situ instruments provide different information, and thus, combining both can improve our understanding of the complex issue of air pollution in the city of Madrid.

Author Contribution

A.S-L. devised the research. D.G-N. and N.B. carried out the measurements and analyzed the data. D.G-N., N.B., R.G. and A.S-L. analyzed and interpreted the results. D.G-N. wrote the manuscript with contributions from all co-authors.

Acknowledgements

The authors want to thank Manuel Perez and David Armenteros for technical assistance with the instrument, and David de la Paz for model assistance. This work was supported by the TECNAIRE project ("Técnicas innovadoras para la evaluación y mejora de la calidad del aire urbano") S2013/MAE-2972. We would also like to thank Juan Ramón Moreta González (PI) and his staff for establishing and maintaining the AERONET sites in Madrid used in this investigation. We acknowledge support of the publication fee by the CSIC Open Access Publication Support Initiative through its Unit of Information Resources for Research (URICI)

References

Ayuntamiento de Madrid (AM): Madrid 2016 Annual Air Quality Assessment Report (Calidad del aire Madrid 2019). General Directorate of Sustainability and Environmental Control, Madrid City Council Available online -only Spanish version- at http://www.mambiente.munimadrid.es/opencms/export/sites/default/calaire/Anexos/Memorias/Memoria_2019.pdf, 2019.

Benavent, N., Garcia-Nieto, D., Wang, S., & Saiz-Lopez, A.: MAX-DOAS measurements and vertical profiles of glyoxal and formaldehyde in Madrid, Spain. Atmospheric Environment, 199, 357-367, 2019.

765

766 Borge, R., Narros, A., Artínano, B., Yagüe, C., et al.: Assessment of
767 micro- scale spatio-temporal variation of air pollution at an urban
768 hotspot in Madrid (Spain) through an extensive field campaign. Atmos.
769 Environ. 140, 432-445, 2016.

770

771 Borge, R., Santiago, J. L., de la Paz, D., Martín, F., Domingo, J.,
772 Valdés, C., Sánchez, B., Rivas, E., Rozas, M. T., Lázaro, S., Pérez,
773 J., & Fernández, Á.: Application of a short term air quality action
774 plan in Madrid (Spain) under a high-pollution episode - Part II:
775 Assessment from multi-scale modelling. Science of the Total
776 Environment, 635, 1574-1584.
777 https://doi.org/10.1016/j.scitotenv.2018.04.323, 2018.

778

779 Carnerero, C., Pérez, N., Reche, C., Ealo, M., Titos, G., Lee, H.-K.,
780 Eun, H.-R., Park, Y.-H., Dada, L., Paasonen, P., Kerminen, V.-M.,
781 Mantilla, E., Escudero, M., Gómez-Moreno, F. J., Alonso-Blanco, E.,
782 Coz, E., Saiz-Lopez, A., Temime-Roussel, B., Marchand, N., Beddows,
783 D. C. S., Harrison, R. M., Petäjä, T., Kulmala, M., Ahn, K.-H.,
784 Alastuey, A., and Querol, X.: Vertical and horizontal distribution of
785 regional new particle formation events in Madrid, Atmos. Chem. Phys.,
786 18, 16601-16618, https://doi.org/10.5194/acp-18-16601-2018, 2018.

787

788 Chan, K. L., Wiegner, M., Alberti, C., & Wenig, M.: MAX-DOAS
789 measurements of tropospheric NO_2 and HCHO in Munich and the comparison
790 to OMI and TROPOMI satellite observations. Atmospheric Measurement
791 Techniques Discussions, 2020.

792

793 Chance, K., Kurucz, R.L.: An improved high-resolution solar reference
794 spectrum for earth's atmosphere measurements in the ultraviolet,
795 visible, and near infrared. J. Quant. Spectrosc. Radiat. Transf.;

Special Issue Dedicated to Laurence S. Rothman on the Occasion of his 70th Birthday 111 (9), 1289-1295, 2010.

Clémer, K., Van Roozendael, M., Fayt, C., Hendrick, F., Hermans, C., Pinardi, G., Spurr, R.,Wang, P., De Mazière, M.: Multiple wavelength retrieval of tropospheric aerosol optical properties from MAXDOAS measurements in Beijing. Atmospheric Measurement Techniques 3 (4), 863, 2010.

Cuevas, C., Notario, A., Adame, J. Hilboll, A., Richter, A., Burrows, J.P, Saiz-Lopez, A.: Evolution of NO2 levels in Spain from 1996 to 2012. Sci Rep 4, 5887, 2014.

de la Paz, D., Borge, R., & Martilli, A.: Assessment of a high resolution annual WRF-BEP/CMAQ simulation for the urban area of Madrid (Spain). Atmospheric Environment, 144, 282-296. https://doi.org/10.1016/j.atmosenv.2016.08.082, 2016.

Dimitropoulou, E., Hendrick, F., Pinardi, G., Friedrich, M., Merlaud, A., Tack, F., De Longueville, H., Fayt, C., Hermans, C., Laffineur, Q., Fierens, F., & Van Roozendael, M.: Validation of TROPOMI tropospheric NO_2 columns using dual-scan MAX-DOAS measurements in Uccle, Brussels. Atmospheric Measurement Techniques Discussions, 2020.

European Environment Agency (EEA).: Air quality in Europe – 2019 report. EEA Technical Report No 10/2019. ISBN: 978-92-9480-088-6. Available online at: http://www.eea.europa.eu/publications/air-quality-in-europe-2019., 2019

Hendrick, F., Müller, J.-., Clémer, K.,Wang, P., De Mazière,M., Fayt, C., Gielen, C., Hermans, C., Ma, J., Pinardi, G., Stavrakou, T., Vlemmix, T., Van Roozendael, M.: Four years of ground-based MAX-DOAS observations of HONO and NO_2 in the Beijing area. Atmos. Chemical Physics, 14 (2), 765, 2014.

Garcia-Nieto, D., Benavent, N., Saiz-Lopez, A.: Measurements of atmospheric HONO vertical distribution and temporal evolution in Madrid (Spain) using the MAXDOAS technique. Science of the Total Environment. 643, 957-966, 2018.

Hönninger, G., von Friedeburg, C., Platt, U.: Multi axis differential optical absorption spectroscopy (MAXDOAS). Atmos. Chem. Phys. 4 (1), 231-254, 2004.

Izquierdo, R., García Dos Santos, S., Borge, R., Paz, D. de la, Sarigiannis, D., Gotti, A., & Boldo, E.: Health impact assessment by the implementation of Madrid City air-quality plan in 2020. Environmental Research, 183, 109021, 2020.

Kramer, L. J., Leigh, R. J., Remedios, J. J., & Monks, P. S: Comparison of OMI and ground-based in situ and MAX-DOAS measurements of tropospheric nitrogen dioxide in an urban area. Journal of Geophysical Research Atmospheres, 2008.

Meller, R., Moortgat, G.K.: Temperature dependence of the absorption cross sections of formaldehyde between 223 and 323 K in the wavelength range 225-375 nm. Journal of Geophysical Research: Atmosphere 105, 7089-7101, 2009.

Monks, P. S., Granier, C., Fuzzi, S., Stohl, A., Williams, M. L., Akimoto, H., Amann, M.,Baklanov, A., Baltensperger, U., Bey, I., Blake, N., Blake, R. S., Carslaw, K., Cooper, O. R., Dentener, F., Fowler, D., Fragkou, E., Frost, G. J., Generoso, S., … von Glasow, R.: Atmospheric composition change - global and regional air quality. Atmospheric Environment, 43(33), 5268-5350. https://doi.org/10.1016/j.atmosenv.2009.08.021, 2009.

Ortega, I., Koenig, T., Sinreich, R., Thomson, D., Volkamer, R.: The CU 2-D-MAX-DOAS instrument – Part 1: Retrieval of 3-D distributions of NO2 and azimuth-dependent OVOC ratios. Atmospheric Measurement Technique, 8, 2371-2395, 2015.

Peters, E., Wittrock, F., GroBmann, K., FrieB, U., Richter, A., Burrows, J.: Formaldehyde and nitrogen dioxide over the remote western Pacific Ocean: SCIAMACHY and GOME-2 validation using ship-based MAX-DOAS observations. Atmospheric Chemistry and Physics. 12 (22), 11179, 2012.

Picornell, M., Ruiz, T., Borge, R. et al. Population dynamics based on mobile phone data to improve air pollution exposure assessments. J Expo Sci Environ Epidemiol 29, 278-291. https://doi.org/10.1038/s41370-018-0058-5, 2019.

Plane, J.M.C., Saiz-Lopez, A.: UV-Visible Differential Optical Absorption Spectroscopy (DOAS). In: Heard, D.E. (Ed.), Analytical Techniques for Atmospheric Measurement. Blackwell Publishing, Oxford, 2006.

884 Platt, U., Stutz, J.: Differential Optical Absorption Spectroscopy:
885 Principles and Applications. Springer Berlin Heidelberg, Berlin,
886 Heidelberg, Berling, Heidelberg, 2008.

887

888 Quaassdorff C, Borge R, Pérez J, Lumbreras J, de la Paz D, de Andrés
889 JM. Microscale traffic simulation and emission estimation in a heavily
890 trafficked roundabout in Madrid (Spain). Sci Total Environ, 566-
891 567:416-427. doi:10.1016/j.scitotenv.2016.05.051, 2016.

892

893 Rodgers, C.D.: Inverse Methods for Atmospheric Sounding: Theory and
894 Practice. World Scientific Publishing, Singapore (Singapore), 2000.

895

896 Rothman, L.S., Gordon, I.E., Barber, R.J., Dothe, H., Gamache, R.R.,
897 Goldman, A., Perevalov, V.L., Tashkum, S.A., Tennyson, J.: HITEMP, the
898 high-temperature molecular spectroscopic database Journal of
899 Quantitative Spectroscopy and Radiative Transfer. 111 (15), 2139,
900 2150, 2010.

901

902 Ryan, R. G., Rhodes, S., Tully, M., Wilson, S., Jones, N., Frieß, U.,
903 and Schofield, R.: Daytime HONO, NO_2 and aerosol distributions from
904 MAX-DOAS observations in Melbourne, Atmos. Chem. Phys., 18, 13969-
905 13985, 2018.

906

907 Saiz-Lopez, A., Borge, R., Notario, A. et al.: Unexpected increase in
908 the oxidation capacity of the urban atmosphere of Madrid, Spain. Sci
909 Rep 7, 45956. https://doi.org/10.1038/srep45956, 2017.

910

911 Schreier, S. F., Richter, A., Peters, E., Ostendorf, M., Schmalwieser,
912 A. W., Weihs, P., & Burrows, J. P: Dual ground-based MAX-DOAS

observations in Vienna, Austria: Evaluation of horizontal and temporal NO2, HCHO, and CHOCHO distributions and comparison with independent data sets. Atmospheric Environment: X 5, 2020

Serdyunchenko, A., Gorshelev, V., Weber, M., Chehade, W., Burrows, J.P.: High spectral resolution ozone absorption cross-sections – Part 2: temperature dependence. Atmospheric Measurement Techniques. 7 (2), 625-636, 2014.

Solomon, S., & Sanders, Ryan W and Schmeltekopf, A. L.: On the Interpretation of Zenith Sky Absorption Measurements. Journal of Geophysical Research, 92, 8311-8319, 1987.

Stutz, J., Kim, E.S., Platt, U., Bruno, P., Perrino, C., Febo, A.: UV-visible absorption cross sections of nitrous acid. Journal of Geophysical Research: Atmosphere. 105, 14585-14592, 2000.

Thalman, R., Volkamer, R.: Temperature dependent absorption cross-sections of O2-O2 collision pairs between 340 and 630 nm and at atmospherically relevant pressure. Physical Chemistry Chemical Physics 15 (37), 15371-15381, 2013.

Vandaele, A.C., Hermans, C., Simon, P.C., Carleer, M., Colin, R., Fally, S., Mérienne, M.F., Jenouvrier, A., Coquart, B.: Measurements of the NO2 absorption cross-section from 42000 cm^-1 to 10000 cm^-2 (238-1000 nm) at 220 K and 294 K. Journal of Quantitative Spectroscopy and Radiative Transfer; Atmospheric Spectroscopy Application 59 (3), 171-184 96, 1998.

Wagner, T., Beirle, S., Benavent, N., Bösch, T., Chan, K. L., Donner, S., Dörner, S., Fayt, C., Frieß, U., García-Nieto, D., Gielen, C., González-Bartolome, D., Gomez, L., Hendrick, F., Henzing, B., Jin, J. L., Lampel, J., Ma, J., Mies, K., Navarro, M., Peters, E., Pinardi, G., Puentedura, O., Puķīte, J., Remmers, J., Richter, A., Saiz-Lopez, A., Shaiganfar, R., Sihler, H., Van Roozendael, M., Wang, Y., and Yela, M.: Is a scaling factor required to obtain closure between measured and modelled atmospheric O4 absorptions? An assessment of uncertainties of measurements and radiative transfer simulations for 2 selected days during the MAD-CAT campaign. Atmospheric Measurement Techniques 12, 2745–2817, 2019.

Schreier, S. F., Richter, A., & Burrows, J. P.: Near-surface and path-averaged mixing ratios of NO2 derived from car DOAS zenith-sky and tower DOAS off-axis measurements in Vienna: A case study. Atmospheric Chemistry and Physics, 2019.

Wang, S., Cuevas, C.A., Frieß, U., Saiz-Lopez, A.: MAX-DOAS retrieval of aerosol extinction properties in Madrid, Spain. Atmospheric Measurement Techniques 9,5089–5101, 2016.

Volkamer, R., Spietz, P., Burrows, J., Platt, U.: High-resolution absorption cross-section of glyoxal in the UV-vis and IR spectral ranges. J. Photochem. Photobiol. Chem. 172 (1), 35-46, 2005.

World Health Statistics (WHO): monitoring health for the SDGs. Wold Health Organization, 2019.

970 Yang, T., Si, F., Luo, Y., Zhan, K., Wang, P., Zhou, H., Zhao, M., &
971 Liu, W.:Source contribution analysis of tropospheric NO_2 based on two-
972 dimensional MAX-DOAS measurements. Atmospheric Environment, 2019.